

Low-PAPR Multi-channel OOK Waveform for IEEE 802.11ba Wake-up Radio

Alphan Şahin, Xiaofei Wang, Hanqing Lou, and Rui Yang

Abstract—The peak-to-average-power ratio (PAPR) of the frequency domain multiplexed wake-up signals (WUSs) specified in IEEE P802.11ba can be very large and difficult to manage since it depends on the number and allocation of the active channels, and the data rate on each channel. To address this issue, we propose a transmission scheme based on complementary sequences (CSs) for multiple WUSs multiplexed in the frequency domain. We discuss how to construct CSs compatible with the framework of IEEE P802.11ba by exploiting a recursive Golay complementary pair (GCP) construction to reduce the instantaneous power fluctuations in time. We compare the proposed scheme with the other options under a non-linear power amplifier (PA) distortion. Numerical results show that the proposed scheme can lower the PAPR of the transmitted signal in frequency division multiple access (FDMA) scenarios more than 3 dB and yields a superior error rate performance under severe PA distortion.

I. INTRODUCTION

A wake-up radio (WUR) is an extremely low-power radio attached to a primary radio. It listens the wireless environment while its primary radio is in sleep mode and wakes it up when there is a packet to receive. Due to its low power consumption, it can potentially reduce the power consumption of the device to maintain the wireless connectivity for many years, which is particularly beneficial for battery-operated and remotely-connected devices [1].

WUR is being discussed under an ongoing IEEE project, i.e., IEEE P802.11ba, which aims at designing Wireless Local Area Network (WLAN) with WUR devices [2]. To enable low-complexity wake-up radio receiver (WURx), an on-off keying (OOK)-based wake-up signal (WUS) has been adopted in IEEE P802.11ba while providing the flexibility for the implementation of the OOK waveform to system designers [2]. In this study, we investigate how to design the OOK-based WUS in frequency division multiple access (FDMA) scenarios under the framework of IEEE P802.11ba.

In the literature, the design of WUS for single channel has been investigated extensively. For example, in [3], OOK signals in a WUS are generated through orthogonal frequency division multiplexing (OFDM) symbols with high-power and low-power constellation points, respectively. In [4], an approach which enables orthogonal multiplexing of WUS and OFDM symbol is proposed. The sequences which lead to ON and OFF signals within the useful duration of OFDM signal are optimized based on several parameters such as peak-to-average-power ratio (PAPR), flatness in frequency, and low leakage on the OFF signals. In [5], simultaneous WUS and

OFDM signal transmission is discussed under the framework of IEEE 802.11ax. To mitigate the interference between WUS and OFDM signal, filtered OOK waveform is proposed. In [6], the concept of partial OOK, which improves the sensitivity performance of a WUR without increasing the complexity, is investigated. There are also other attempts to generate a low data rate WUS by exploiting the existing IEEE 802.11 amendments. For example, in [7], special bit streams which purposely yield to OFDM symbols with high PAPRs in IEEE 802.11a/g/n packets are proposed. The location of the peak sample is controlled in time by using different bit streams for WUS. Mapping the low-power constellation points to the lower half of the channel bandwidth, and high-power points to the upper half to encode a bit 0 (and vice versa for bit 1), i.e., frequency-shift keying (FSK), is also another strategy mentioned in [7]. In [8] and [9], the information bits related to WUS are encoded with the frame length by using multiple consecutive Wi-Fi or Bluetooth Low Energy (BLE) packets. A comprehensive survey on other modulation techniques for WURs can be found in [10]. To the best of our knowledge, the design of OOK waveform in FDMA scenarios has not been investigated rigorously yet.

One of the main challenges to design an OOK waveform applicable in FDMA scenarios [2] is the large instantaneous power fluctuation. To address this issue, we first propose a transmission scheme which unifies the low data rate (LDR) WUS and the high data rate (HDR) WUS generation methods. We then generate OOK waveform based on complementary sequences (CSs) to limit the PAPR below 3 dB. We show how to construct CSs compatible with FDMA in IEEE P802.11ba by exploiting a recursive Golay complementary pair (GCP) construction. We compare the proposed scheme with the other options provided in [2] under non-linear power amplifier (PA) distortion.

Notation: The field of complex numbers, the set of integers, the set of positive integers, and the set of non-negative integers are denoted by \mathbb{C} , \mathbb{Z} , \mathbb{Z}^+ , and \mathbb{Z}_0^+ respectively. The symbol $*$ denotes convolution operation. The symbols i , j , $+$, and $-$ denote $\sqrt{-1}$, $-\sqrt{-1}$, 1 , and -1 , respectively. The Hermitian operation and the complex conjugation are denoted by $(\cdot)^H$ and $(\cdot)^*$ respectively. The operator $\tilde{\mathbf{a}}$ reverses the order of the elements of the sequence \mathbf{a} and applies element-wise complex conjugation. The operation $\uparrow_k \{\mathbf{a}\}$ introduces $k - 1$ zero symbols between the elements of \mathbf{a} .

II. IEEE P802.11BA FRAMEWORK

In the current draft of IEEE P802.11ba [2], a WUS is based on 4 MHz OOK waveform. While the ON and OFF signal

durations are set to be $4 \mu\text{s}$ for LDR WUS, they are $2 \mu\text{s}$ for HDR WUS, which are half of the IEEE 802.11n/ac OFDM symbol duration. To enable non-coherent detection, the bits for the payload are encoded with a Manchester-like encoding, called *WUR encoding*. The WUR encoding is defined as $[1 \ 0]$ and $[0 \ 1]$ for bit 0 and bit 1 for HDR, and $[1 \ 0 \ 1 \ 0]$ and $[0 \ 1 \ 0 \ 1]$ for bit 0 and bit 1 for LDR, respectively. Hence, the data rates for the WUSs for HDR and LDR correspond to 250 kbit/s or 62.5 kbit/s, respectively.

The current draft of the standard provides several ways of generating the OOK waveform. For example, using the half duration of the 802.11n/ac OFDM symbols with 12 non-zero subcarriers and 1 zero center tone (i.e., masked-based approach) or using a smaller inverse discrete Fourier transform (IDFT) with 6 non-zero subcarriers and 1 zero center tone are two of the exemplified methods to generate the ON signals for HDR WUS. The LDR WUS is suggested to be generated by using the same signal processing operation for HDR, i.e., OFDM with 12 non-zero subcarriers and 1 zero center tone.

A WUS can cause spikes on certain frequency tones if identical ON signals are used repeatedly. However, according to Federal Communications Commission (FCC) Part 15.247 regulations, the maximum power in any 3 kHz band should be less than 8 dBm during any time interval of continuous transmission [11]. Hence, the coverage range of such a WUS would be limited. To avoid this issue, IEEE P802.11ba adopts a signal randomization method where the output of IDFT is rotated cyclically. The amount of the rotation is based on 8 uniformly separated values within the IDFT duration and determined with a linear feedback shift register (LFSR).

To maintain the coexistence between different IEEE 802.11 devices at the same location, the WUS starts with the 802.11a/g preamble (legacy fields), i.e., short training field (STF), long training field (LTF), and a signal field (SIG). In addition, the legacy fields are appended with two spoofing symbols, i.e., BPSK mark, and a SYNC field for synchronization at the WURx, where its duration is either $64 \mu\text{s}$ and $128 \mu\text{s}$ for HDR and LDR, respectively. The SYNC field is constructed based on HDR OOK waveform for both HDR and LDR WUSs. No WUR encoding is applied for the SYNC field. A binary sequence of length 32 is utilized for the SYNC field for HDR WUS. The same binary sequence is repeated and inverted for the SYNC field of LDR WUS [12].

In IEEE P802.11ba, multiplexing WUSs within 20 MHz is not allowed. However, WUSs with different data rates can be multiplexed optionally within $2 \times 20 \text{ MHz}$ or $4 \times 20 \text{ MHz}$ where each 20 MHz channel can have a single 4 MHz WUS. When WUSs are multiplexed in the frequency domain, the ON signals on different channels overlap in time domain. Thus, without any precaution, the multi-channel operation can cause fluctuation in time domain and decrease the coverage range. To mitigate the fluctuations, phase rotations on different channels, as described in IEEE 802.11ac [13], are adopted. However, this may not be an effective method as the number of active channels changes based on the encoded bits on different channels. In addition, the number of possible signals for each $4 \mu\text{s}$ grows exponentially with the number of active channels in case of FDMA due to the random cyclic shifts in time.

III. PRELIMINARIES AND FURTHER NOTATION

We define the polynomial representation of the sequence \mathbf{a} of length L_s as

$$p_{\mathbf{a}}(z) \triangleq a_{L_s-1}z^{L_s-1} + a_{L_s-2}z^{L_s-2} + \dots + a_0, \quad (1)$$

where $z \in \mathbb{C}$ is a complex number. The polynomial $p_{\mathbf{a}}(z^k)$, $p_{\mathbf{a}}(z^k)p_{\mathbf{b}}(z^l)$, and $p_{\mathbf{a}}(z)z^m$ represent the up-sampled sequence \mathbf{a} with the factor of $k \in \mathbb{Z}^+$, the convolution of the up-sampled sequence \mathbf{a} by k and the up-sampled sequence \mathbf{b} by $l \in \mathbb{Z}^+$, and the sequence \mathbf{a} padded with $m \in \mathbb{Z}_0^+$ zero symbols, respectively. The polynomial $p_{\mathbf{a}}(z)$ corresponds to an OFDM symbol in continuous time when z is restricted to be on the unit circle in the complex plane, i.e., $z \in \{e^{j\frac{2\pi t}{T_s}} \mid 0 \leq t < T_s\}$, where the subcarriers are modulated with the elements of the sequence \mathbf{a} , and T_s denotes the OFDM symbol duration.

The sequence pair (\mathbf{a}, \mathbf{b}) is called a GCP if

$$p_{\mathbf{a}}(z)p_{\mathbf{a}^*}(z^{-1}) + p_{\mathbf{b}}(z)p_{\mathbf{b}^*}(z^{-1}) = \rho_{\mathbf{a}}(0) + \rho_{\mathbf{b}}(0), \quad (2)$$

where $\rho_{\mathbf{a}}(k)$ and $\rho_{\mathbf{b}}(k)$ is the aperiodic auto correlation (APAC) coefficient of the sequence \mathbf{a} and \mathbf{b} , respectively. Each sequence in a GCP is a CS [14]. The CSs are first proposed in [14] in 1961. The CS construction methods have been extensively studied in the literature (see [15] and the references therein). One of the most appealing features of a CS is the low instantaneous peak power when the sequence is transmitted with an OFDM symbol. If \mathbf{a} is also a unimodular CS, i.e., $|a_i| = |a_j|$ for $i \neq j$, one can show that the PAPR of the corresponding OFDM symbols is less than or equal to 2.

In [16], a generalized version of Golay's concatenation and interleaving methods is restated by the following theorem:

Theorem 1. *Let (\mathbf{a}, \mathbf{b}) and (\mathbf{c}, \mathbf{d}) be GCPs of length L_s and M , respectively, and $\omega_1, \omega_2 \in \{u : u \in \mathbb{C}, |u| = 1\}$ and $k, l, m \in \mathbb{Z}$. Then, the sequences \mathbf{f} and \mathbf{g} with their polynomial representations given by*

$$p_{\mathbf{f}}(z) = \omega_1 p_{\mathbf{a}}(z^k) p_{\mathbf{c}}(z^l) + \omega_2 p_{\mathbf{b}}(z^k) p_{\mathbf{d}}(z^l) z^m, \quad (3)$$

$$p_{\mathbf{g}}(z) = \omega_1 p_{\mathbf{a}}(z^k) p_{\bar{\mathbf{c}}}(z^l) - \omega_2 p_{\mathbf{b}}(z^k) p_{\bar{\mathbf{d}}}(z^l) z^m, \quad (4)$$

construct a GCP.

The proof for Theorem 1 is given in [16] by using the definition given in (2).

IV. GOLAY-BASED MULTI-CHANNEL OOK WAVEFORM

In this section, we discuss a simple transmitter structure for generating ON signals on different channels for both HDR and LDR WUSs. By using this structure and exploiting GCPs, we show how to control the PAPR of the signal regardless of the data rate of WUS on different channels and signal randomization discussed in Section II.

A. Aligning the OFDM symbol boundaries for LDR and HDR

To reduce the number of possible signals for each $4 \mu\text{s}$ in case of HDR and LDR WUSs multiplexing, we first align the OFDM symbol periods for LDR and HDR by constructing each ON duration of the LDR WUS with two HDR ON signals transmitted back-to-back. For example, consider a

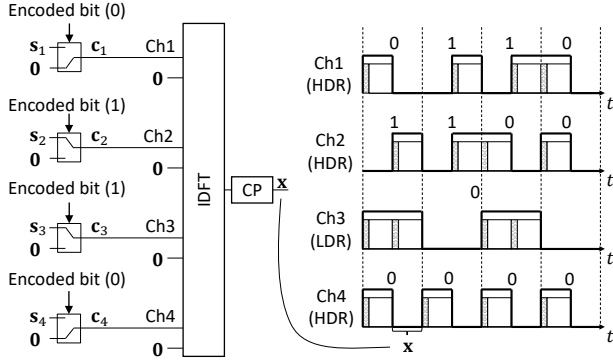


Figure 1. Supporting LDR and HDR WUSs with single OFDM transmitter.

multi-channel operation where the first two channels and the fourth channel carry HDR WUS and the third channel carries LDR WUS as in Figure 1. Each ON signal for LDR WUS on the third channel consists of two HDR ON signal, in which the second OFDM symbol can be a repetition of the first OFDM symbol or another OFDM symbol generated through a different sequence. As shown in Figure 1, this approach aligns the symbol boundaries of the OFDM symbols in time for different channels. The alignment is beneficial to adjust the sequences on each channel to control the PAPR level of the combined signal in case of FDMA transmission of mixed LDR and HDR WUSs. In addition, the random cyclic shifts at the IDFT output do not change the PAPR properties of the generated signal. Note that this approach can also be expressed as a different WUR encoding for LDR case. For example, bit 0 and bit 1 may be encoded as [1 1 0 0 1 1 0 0] and [0 0 1 1 0 0 1 1] for LDR before the OOK waveform generation, respectively. Hence, the ON and OFF durations for LDR are set effectively to the ones used for HDR.

Let b_i be the encoded bit and $\mathbf{c}_i \in \mathbb{C}^{L \times 1}$ be the sequence utilized in frequency for the i th channel. If $b_i = 1$, $\mathbf{c}_i = \mathbf{s}_i \in \mathbb{C}^{L \times 1}$, otherwise it is set to a zero vector. Considering four channels, the OFDM symbol in the baseband $\mathbf{x} \in \mathbb{C}^{N \times 1}$ can be expressed as $\mathbf{x} = \mathbf{A} \mathbf{F}_N^H \mathbf{M} [\mathbf{c}_1^H \ \mathbf{c}_2^H \ \mathbf{c}_3^H \ \mathbf{c}_4^H]^H$, where $\mathbf{A} \in \mathbb{C}^{(N+N_{cp}) \times N}$ is a matrix that appends the cyclic prefix (CP) to the beginning of the symbol, $\mathbf{F}_N \in \mathbb{C}^{N \times N}$ is the discrete Fourier transform (DFT) matrix, and $\mathbf{M} \in \mathbb{C}^{N \times 4L}$ is the mapping matrix that maps \mathbf{c}_i to the i th channel for $i = 1, 2, 3, 4$. The transmitter diagram is illustrated in Figure 1. In one implementation, N and N_{cp} can be set to 128 and 16 for 80 MHz sample rate. Hence, \mathbf{x} will be transmitted within $2 \mu\text{s}$, which is equivalent to ON duration for HDR WUS. If $\mathbf{c}_i = \mathbf{s}_i$, the i th channel is activated for $2 \mu\text{s}$. If it is activated twice, the ON duration for LDR WUS is generated on i th channel. In the following subsection, we discuss the design of \mathbf{s}_i for $i = 1, 2, 3, 4$.

B. Golay-based Multi-channel OOK Waveform

The parameters k and l upsample the sequences in Theorem 1 while the parameter m separates the corresponding sequences by padding zeros. Since the parameter m can be an arbitrary value, Theorem 1 gives flexibility to control the

PAPR of a signal for non-contiguous resource allocation. In this study, we exploit this property to mitigate the PAPR of a signal which consists of multiple ON signals in different channels while maintaining zero center tone (e.g., DC tone) on each channel.

Let \mathbf{a} and \mathbf{b} be a GCP of length L_s , $\mathbf{c} = \mathbf{d} = \mathbf{1}$, $k = l = 1$, and $m = L_s + 1$. Based on (3) and (4), the corresponding sequences in the GCPs can be obtained as

$$\mathbf{f}_1 = (\omega_1 \times \mathbf{a}, 0, \omega_2 \times \mathbf{b}) \quad (5)$$

$$\mathbf{g}_1 = (\omega_1 \times \mathbf{a}, 0, -\omega_2 \times \mathbf{b}) \quad (6)$$

Similarly, by alternating the variables in Theorem 1, $\mathbf{f} = (\omega_1 \times \mathbf{a}, 0, \omega_2 \times \mathbf{b})$ and $\mathbf{g} = (\omega_1 \times \tilde{\mathbf{a}}, 0, -\omega_2 \times \tilde{\mathbf{b}})$ also construct a GCP. Hence, by choosing $L_s = 3$ and $\omega_1 = \omega_2 = 1$, a set of CSs with zero center tone and compatible with IEEE P802.11ba OOK waveform can be generated. For example, let $\mathbf{a} = (+, i, +)$ and $\mathbf{b} = (+, +, -)$ based on the GCP lists provided in [17]. By utilizing (5) and (6), \mathbf{f}_1 and \mathbf{g}_1 are obtained as $\mathbf{f}_1 = (+, i, +, 0, +, +, -)$ and $\mathbf{g}_1 = (+, i, +, 0, -, -, +)$ and they can be used for generating $2 \mu\text{s}$ ON signal with the transmitter structure in Figure 1. To utilize \mathbf{f}_1 and \mathbf{g}_1 for multi-channel operations, the following rules may be considered:

1) *Case I (The number of active channels is 1):* When only one of the channels is active, either $\mathbf{f}_1 = (\mathbf{a}, 0, \mathbf{b})$ and $\mathbf{g}_1 = (\mathbf{a}, 0, -\mathbf{b})$ can be mapped to the inputs of IDFT to generate ON signal for the corresponding channel. Since \mathbf{f}_1 and \mathbf{g}_1 are the unimodular CSs, they lead to the OFDM signals where their PAPRs are less than 3 dB.

2) *Case II (The number of active channels is 2):* The sequences \mathbf{f}_1 and \mathbf{g}_1 construct GCP. Therefore, \mathbf{f}_1 and \mathbf{g}_1 can be re-used in (3) and (4) to form larger CSs. For $\omega_1 = \omega_2 = 1$, the new pair can be obtained as

$$\mathbf{f}_2 = (\mathbf{f}_1, \mathbf{0}_m, \mathbf{g}_1) = (\mathbf{a}, 0, \mathbf{b}, \mathbf{0}_m, \mathbf{a}, 0, -\mathbf{b}) \quad (7)$$

$$\mathbf{g}_2 = (\mathbf{f}_1, \mathbf{0}_m, -\mathbf{g}_1) = (\mathbf{a}, 0, -\mathbf{b}, \mathbf{0}_m, -\mathbf{a}, 0, \mathbf{b}) \quad (8)$$

by using the same rationale in (5) and (6), where m can be chosen arbitrarily. In other words, the sequences \mathbf{f}_1 and \mathbf{g}_1 can be mapped to different channels regardless of the separation between the channels in frequency without affecting the PAPR. For example, the sequences \mathbf{f}_1 and \mathbf{g}_1 can be utilized to generate ON signals for any two of the four channels. Note that \mathbf{f}_1 and \mathbf{g}_1 can also be manipulated based on Theorem 1 before mapping to the subcarriers. For example, one channel can utilize the sequence $j \times \mathbf{f}_1$ while the other channel may utilize the sequence $i \times \mathbf{g}_1$, i.e., $\omega_1 = j$ and $\omega_2 = i$.

3) *Case III (The number of active channels is 3):* For this case, either three contiguous channels or the first, second (or third), and the fourth channels are active at the same time. To address the first scenario, let $l = 1$, $\mathbf{c} = \mathbf{a}$, and $\mathbf{d} = \mathbf{b}$. The generated sequences based on Theorem 1 can be expressed as $\mathbf{f}_3 = (\uparrow_k \{\mathbf{a}\} * \mathbf{a}, \mathbf{0}_m) + (\mathbf{0}_m, \uparrow_k \{\mathbf{b}\} * \mathbf{b})$ and $\mathbf{g}_3 = (\uparrow_k \{\mathbf{a}\} * \tilde{\mathbf{b}}, \mathbf{0}_m) - (\mathbf{0}_m, \uparrow_k \{\mathbf{b}\} * \tilde{\mathbf{a}})$. If $m = L_s + 1$ and $k \geq 2L_s + 1$, the sequences which cover three contiguous channels can be formed by using a GCP of length 3. For example, if $\mathbf{a} =$

Table I
SEQUENCES FOR MULTI-CHANNEL OOK WAVEFORM

b_1, b_2, b_3, b_4	\mathbf{c}_1	\mathbf{c}_2	\mathbf{c}_3	\mathbf{c}_4
0000	$\mathbf{0}_L$	$\mathbf{0}_L$	$\mathbf{0}_L$	$\mathbf{0}_L$
1000	$(\mathbf{a}, 0, \mathbf{b})$	$\mathbf{0}_L$	$\mathbf{0}_L$	$\mathbf{0}_L$
0100	$\mathbf{0}_L$	$(\mathbf{a}, 0, \mathbf{b})$	$\mathbf{0}_L$	$\mathbf{0}_L$
1100	$(\mathbf{a}, 0, \mathbf{b})$	$(\mathbf{a}, 0, -\mathbf{b})$	$\mathbf{0}_L$	$\mathbf{0}_L$
0010	$\mathbf{0}_L$	$\mathbf{0}_L$	$(\mathbf{a}, 0, -\mathbf{b})$	$\mathbf{0}_L$
1010	$(\mathbf{a}, 0, \mathbf{b})$	$\mathbf{0}_L$	$(\mathbf{a}, 0, -\mathbf{b})$	$\mathbf{0}_L$
0110	$\mathbf{0}_L$	$(\mathbf{a}, 0, \mathbf{b})$	$(\mathbf{a}, 0, -\mathbf{b})$	$\mathbf{0}_L$
1110	$(\mathbf{a}, 0, \mathbf{b})$	$(\mathbf{ia}, 0, \mathbf{b})$	$(\mathbf{a}, 0, -\mathbf{b})$	$\mathbf{0}_L$
0001	$\mathbf{0}_L$	$\mathbf{0}_L$	$\mathbf{0}_L$	$(\mathbf{a}, 0, \mathbf{b})$
1001	$(\mathbf{a}, 0, \mathbf{b})$	$\mathbf{0}_L$	$\mathbf{0}_L$	$(\mathbf{a}, 0, -\mathbf{b})$
0101	$\mathbf{0}_L$	$(\mathbf{a}, 0, \mathbf{b})$	$\mathbf{0}_L$	$(\mathbf{a}, 0, -\mathbf{b})$
1101*	$(\mathbf{a}, 0, \mathbf{b})$	$(\mathbf{ia}, 0, \mathbf{b})$	$\mathbf{0}_L$	$(\mathbf{a}, 0, -\mathbf{b})$
0011	$\mathbf{0}_L$	$\mathbf{0}_L$	$(\mathbf{a}, 0, \mathbf{b})$	$(\mathbf{a}, 0, -\mathbf{b})$
1011*	$(\mathbf{a}, 0, \mathbf{b})$	$\mathbf{0}_L$	$(\mathbf{ja}, 0, -\mathbf{b})$	$(\mathbf{a}, 0, -\mathbf{b})$
0111	$\mathbf{0}_L$	$(\mathbf{a}, 0, \mathbf{b})$	$(\mathbf{ia}, 0, \mathbf{b})$	$(\mathbf{a}, 0, -\mathbf{b})$
1111	$(\mathbf{a}, 0, \mathbf{b})$	$(\mathbf{a}, 0, -\mathbf{b})$	$(-\mathbf{a}, 0, -\mathbf{b})$	$(-\mathbf{a}, 0, \mathbf{b})$

$(+, i, +)$ and $\mathbf{b} = (+, +, -)$, for $\omega_1 = \omega_2 = 1$, \mathbf{f}_3 and \mathbf{g}_3 can be obtained as

$$\mathbf{f}_3 = (\mathbf{a}, 0, \mathbf{b}, \mathbf{0}_{k-2L_s-1}, \mathbf{ia}, 0, \mathbf{b}, \mathbf{0}_{k-2L_s-1}, \mathbf{a}, 0, -\mathbf{b}) , \quad (9)$$

$$\mathbf{g}_3 = (\mathbf{a}, 0, -\mathbf{b}, \mathbf{0}_{k-2L_s-1}, \mathbf{ia}, 0, -\mathbf{b}, \mathbf{0}_{k-2L_s-1}, \mathbf{a}, 0, \mathbf{b}) . \quad (10)$$

By using (9), the ON duration for the first, the second, and the third channel can be generated by using $(\mathbf{a}, 0, \mathbf{b})$, $(\mathbf{ia}, 0, \mathbf{b})$, and $(\mathbf{a}, 0, -\mathbf{b})$ (or $(\mathbf{a}, 0, -\mathbf{b})$, $(\mathbf{ia}, 0, -\mathbf{b})$, and $(\mathbf{a}, 0, \mathbf{b})$ based on (10)), respectively. Unfortunately, to the best of our knowledge, Theorem 1 does not yield CS with quadrature phase shift keying (QPSK) alphabet when the active channels are not contiguous. In this study, we use $(\mathbf{a}, 0, \mathbf{b})$ and $(\mathbf{a}, 0, -\mathbf{b})$ for the first and second channel, respectively, and choose ω_1 and ω_2 from QPSK alphabet for the sequence $(\omega_1 \times \mathbf{a}, 0, -\omega_2 \times \mathbf{b})$ for the third (or the second) channel to minimize PAPR while maintaining the dynamic range for each individual channel low and decreasing the transmitter complexity.

4) *Case IV (The number of active channels is 4)*: This case can be addressed by utilizing Theorem 1 and exploiting the GCP of \mathbf{f}_2 and \mathbf{g}_2 . For $\omega_1 = \omega_2 = 1$, the sequences can be obtained as

$$\mathbf{f}_3 = (\mathbf{f}_2, \mathbf{0}_m, \mathbf{g}_2) = (\mathbf{f}_1, \mathbf{0}_m, \mathbf{g}_1, \mathbf{0}_m, \mathbf{f}_1, \mathbf{0}_m, -\mathbf{g}_1) , \quad (11)$$

$$\mathbf{g}_3 = (\mathbf{f}_2, \mathbf{0}_m, -\mathbf{g}_2) = (\mathbf{f}_1, \mathbf{0}_m, \mathbf{g}_1, \mathbf{0}_m, -\mathbf{f}_1, \mathbf{0}_m, \mathbf{g}_1) . \quad (12)$$

Thus, the first, the second, the third, and the fourth channels can utilize \mathbf{f}_1 , \mathbf{g}_1 , \mathbf{f}_1 and $-\mathbf{g}_1$ (or \mathbf{f}_1 , \mathbf{g}_1 , $-\mathbf{f}_1$ and \mathbf{g}_1), respectively, as indicated in (9), to maintain the PAPR less than 3 dB even though the four channels are active simultaneously.

In Table I, the sequences for given active channels in one OFDM symbol duration are listed. Other than the cases indicated by * in Table I, i.e., $(b_1, b_2, b_3, b_4) = (1, 1, 0, 1)$ and $(b_1, b_2, b_3, b_4) = (1, 0, 1, 1)$, the sequences \mathbf{c}_i for $i = 1, 2, 3, 4$ form a CS when they mapped to the channels and the PAPR of the corresponding signal is less than or equal to 3 dB. In addition, the dynamic range for each channel is also limited since \mathbf{c}_i itself is a CS for $i = 1, 2, 3, 4$. Another observation from Table I is that the sequence in one channel changes based on the transmitted bits on the other channels. However, since WURx is expected to be a simple OOK receiver, e.g., envelope detector, this is not an issue for WURx.

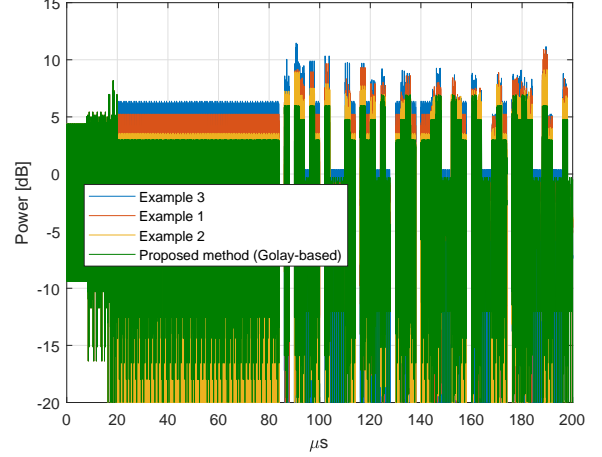


Figure 2. Temporal characteristics of IEEE P802.11ba signal when two LDR and two HDR WUSs are multiplexed in frequency.

V. NUMERICAL RESULTS

We set the sampling rate to 320 MHz for the simulation, which is sufficient to reveal time-domain characteristics. For the PA model, we consider Rapp model with a smoothness factor of 3. For WURx, we consider an envelope detector where the received samples are accumulated as the sum of absolutes of I- and Q-branches. We utilize a 5th order Butterworth low-pass filter as the receive filter whose bandwidth is 5 MHz. We assume ideal synchronization. For the proposed scheme (Golay-based), we consider the CSs given in Table I, where $\mathbf{a} = (+, i, +)$ and $\mathbf{b} = (+, +, -)$ [17]. We compare the proposed scheme with the three examples provided and denoted as Example 1-3 in [2]. For Example 1-3, the length 7 sequences and the length 13 sequences are mapped to the corresponding inputs of IDFT. The $2 \mu\text{s}$ and $4 \mu\text{s}$ ON signals for HDR and LDR are generated after $0.4 \mu\text{s}$ and $0.8 \mu\text{s}$ CP are appended to $1.6 \mu\text{s}$ and $3.2 \mu\text{s}$ IDFT outputs, respectively. We also apply phase rotations for the channels as described in IEEE 802.11ac [13] for Example 2-4. The phase rotations are not applied for the proposed method. To avoid spikes in frequency due to the OOK waveform, we consider time domain cyclic shifts for HDR and LDR ON signals, where the amount of the cyclic shifts are chosen randomly from 8 uniformly separated values within the $1.6 \mu\text{s}$ and $3.2 \mu\text{s}$ IDFT durations, respectively. For the proposed method, we cyclically shift the output of IDFT.

A. Temporal Characteristics

In Figure 2, we provide the snapshots for IEEE P802.11ba packets generated through different options. In this analysis, while the first two channels carry HDR WUSs, the last two channels are loaded with two LDR WUSs. The average power is set to 1. The first $20 \mu\text{s}$ consist of the legacy fields. The following $64 \mu\text{s}$ is the combination of the SYNC fields for LDR and HDR WUSs. The subsequent $64 \mu\text{s}$ includes the combination of the OOK signals at the SYNC fields for the LDR and HDR WUSs. Figure 2 shows that the instantaneous power for Example 2-4 can be $11 - 11.5 \text{ dB}$ and $4 - 5 \text{ dB}$

Table II
PAPR PERFORMANCE AT DIFFERENT PERCENTILES FOR DIFFERENT SCENARIOS (H: HDR, L: LDR, X: NONE)

Rates: Percentile:	Case I [dB]			Case II [dB]			Case III [dB]			Case IV [dB]			Case V [dB]		
	X	X	H H	H	H	H	L	L	H H	L	L	L H	H	H	L H
Golay-based	0.5	0.8	0.99	0.5	0.8	0.99	0.5	0.8	0.99	0.5	0.8	0.99	0.5	0.8	0.99
Example 2	6.58	6.59	6.61	7.09	7.10	7.13	7.09	8.04	9.61	7.22	9.25	9.87	7.09	9.14	9.60
Example 3	9.31	9.42	9.55	9.86	12.34	12.53	8.90	9.43	11.48	8.71	9.41	11.30	9.40	10.98	11.89
Example 1	8.21	8.32	8.49	8.73	8.83	8.94	8.24	8.74	10.94	8.11	9.37	11.00	8.63	10.09	11.17

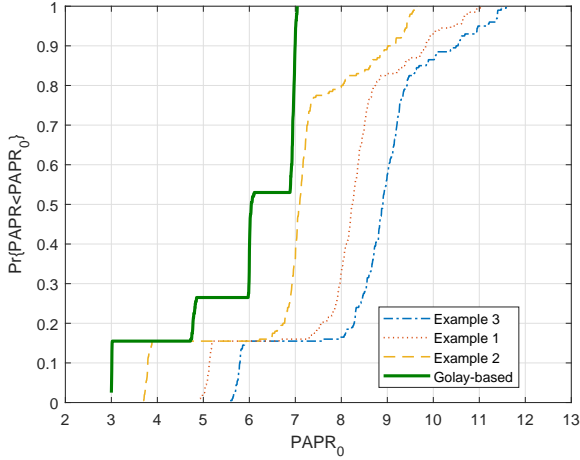


Figure 3. PAPR distribution.

higher than the average power and the instantaneous power for the legacy header, respectively. We observe that Example 3 causes the highest fluctuations, whereas the proposed method mitigates them substantially. Figure 2 also shows that the instantaneous power level with the proposed method is similar to that of the legacy SIG and random cyclic shifts do not alter the variation of the signals.

B. PAPR Results and Spectral Regrowth

In Figure 3, we compare the PAPR distributions for different options. We consider the same setup as given for Figure 2, i.e., two HDR WUSs and two LDR WUSs. We measure the PAPR for each $4 \mu\text{s}$. The results are aligned with the temporal characteristics given in Figure 2. While the PAPRs can reach to 9.5, 11.5 and 11 dB for Example 2, Example 3, and Example 1, respectively, the PAPR is limited to 7 dB in the worst case for the proposed method. In other words, the proposed method provides 3.5, 4.5, and 4 dB PAPR gain as compared to Example 2, Example 3, and Example 1, respectively, for this scenario. In Table II, we also provide PAPR at %50, %80, and %99 percentiles at cumulative distribution function (CDF) curves for different configurations. The results show gains in PAPR for all scenarios.

In Figure 4, we analyze the spectral regrowth under the distortion due to the PA non-linearity. For this analysis, we consider a pessimistic scenario where an access point (AP) wakes up the far stations. We assume that all the channels carry LDR WUSs. We set the output back-off (OBO) as 5 dB. Hence, the P802.11ba packet experiences a heavy distortion. Under this stress test, Example 3 does not satisfy the 802.11 80 MHz spectral emission mask (SEM) while Example 2 and

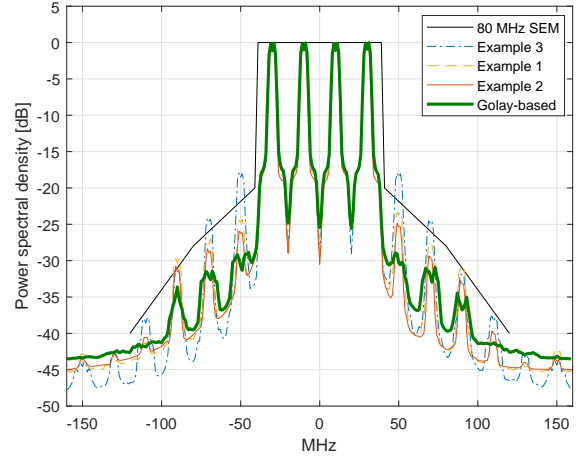


Figure 4. Spectral regrowth (OBO = 5 dB).

Example 1 do not provide room for the spectral regrowth. On the other hand, the proposed method still provides a notable margin under heavy distortion, which indicates robustness against distortion due to the PA non-linearity. Hence, the proposed scheme can yield a higher coverage as compared to that of other options under practical scenarios.

C. BER Results

In Figure 5 and Figure 6, we provide the bit error rate (BER) results for an additive white Gaussian noise (AWGN) channel. For the configuration, we consider two HDR WUSs and two LDR WUSs are multiplexed in frequency. Without taking the distortion due to the PA into account, the OOK waveform with the lowest PAPR for single channel, i.e., Example 2, performs slightly better than the others as in Figure 5. This is because that WURx accumulates the sum of the absolute value of the received samples. Nevertheless, the difference among the options is negligible. When heavy PA distortion is considered, the PAPR of the overall signal becomes more important than the fluctuations within one channel. The OOK waveform with better PAPR also exhibits a better BER performance as in Figure 6. While the degradation due to the distortion is negligible for the proposed method for both LDR and HDR WUSs, 0.5 – 1.5 dB degradation in BER is observed for the other options, particularly Example 3. The similar results are also obtained under a fading channel as illustrated in Figure 7, where the fading channel model is HyperLAN-A. Note that the LDR and HDR reference curves are based on the result for the proposed method without PA impairments and included in Figure 6 and Figure 7 for the sake of comparison.

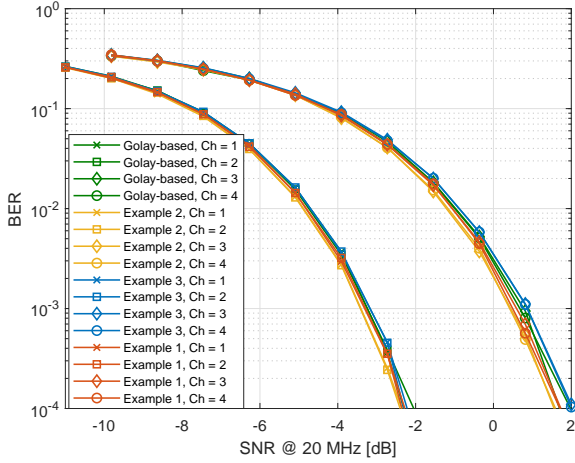


Figure 5. AWGN BER performance without PA.

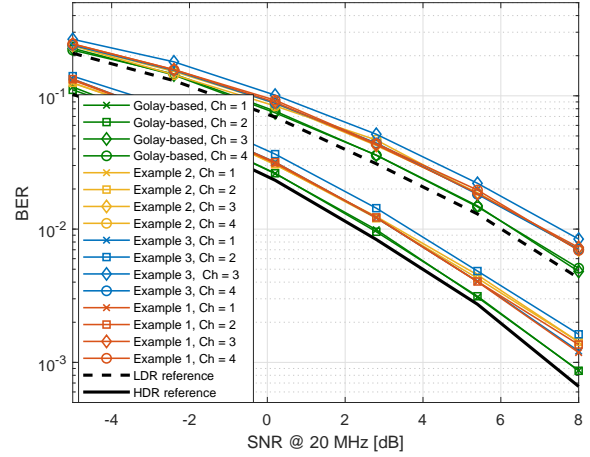


Figure 7. BER under fading channel and PA impairment (OBO = 5).

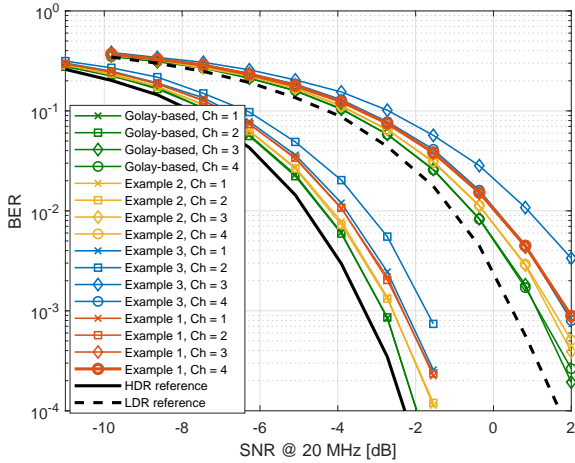


Figure 6. BER under AWGN channel and PA impairment (OBO = 5).

VI. CONCLUDING REMARKS

The PAPR can be large when WUSs are multiplexed in the frequency domain. Without taking any precautions, the instantaneous peak power can reach 10-12 dB higher than the average power, which can limit the coverage range for WUS. The PAPR minimization for multiplexed WUSs is a challenging problem due to the large number of possible cases in an FDMA scenario for IEEE P802.11ba and the simple phase rotations in IEEE 802.11ac cannot address all cases. We show that the existing CSs can address the PAPR issue in the majority of the cases as the corresponding signals are always bounded by 3 dB and the PAPR gain can reach more than 3 dB in some cases by using known CSs as compared to the example sequences in [2].

Although our evaluation shows notable improvement in terms of PAPR for P802.11ba FDMA, which has only four channels, how to construct multi-channel OOK waveform for any given number of channels still needs to be investigated. In addition, we observe that there may be cases (e.g., when the active channels are asymmetrically located in frequency) where there are no CSs with QPSK alphabet. Hence, another

interesting investigation can be an extension to these asymmetric cases to complete the proposed scheme.

REFERENCES

- [1] D. K. McCormick, "IEEE technology report on wake-up radio: An application, market, and technology impact analysis of low-power/low-latency 802.11 wireless LAN interfaces," pp. 1–56, Nov 2017.
- [2] "Part 11: Wireless LAN medium access control (MAC) and physical layer (PHY) specifications amendment: Wake-up radio operation, Amendment 9: Wake-up radio operation," IEEE P802.11ba/D2.0, 2019.
- [3] H. Zhang, C. Li, S. Chen, X. Tan, N. Yan, and H. Min, "A low-power OFDM-based wake-up mechanism for IoE applications," *IEEE Trans. Circuits Syst. II, Express Briefs*, vol. 65, no. 2, pp. 181–185, Feb 2018.
- [4] A. Sahin and R. Yang, "Sequence-based OOK for orthogonal multiplexing of wake-up radio signals and OFDM waveforms," in *Proc. IEEE Global Telecommunications Conf. (GLOBECOM)*, Dec 2018, pp. 1–5.
- [5] L. R. Wilhelmsson, M. M. Lopez, S. Mattisson, and T. Nilsson, "Spectrum efficient support of wake-up receivers by using (O)FDMA," in *Proc. IEEE Wireless Communications and Networking Conference (WCNC)*, April 2018, pp. 1–6.
- [6] D. Sundman, M. M. Lopez, and L. R. Wilhelmsson, "Partial on-off keying - a simple means to further improve IoT performance," in *Proc. IEEE Global Internet of Things Summit (GloTS)*, June 2018, pp. 1–5.
- [7] H. S. Kim and D. D. Wentzloff, "Back-channel wireless communication embedded in WiFi-compliant OFDM packets," *IEEE J. Sel. Areas Commun.*, vol. 34, no. 12, pp. 3181–3194, Dec. 2016.
- [8] S. Tang, H. Yomo, and Y. Takeuchi, "Optimization of frame length modulation-based wake-up control for green WLANs," *IEEE Trans. Veh. Technol.*, vol. 64, no. 2, pp. 768–780, Feb 2015.
- [9] N. E. Roberts *et al.*, "A 236nw -56.5dBm-sensitivity Bluetooth low-energy wakeup receiver with energy harvesting in 65nm CMOS," in *Proc. IEEE Int. Solid-State Circuits Conf.*, Jan 2016, pp. 450–451.
- [10] R. Piyare *et al.*, "Ultra low power wake-up radios: A hardware and networking survey," *IEEE Commun. Surveys Tut.*, vol. 19, no. 4, pp. 2117–2157, Fourth quarter 2017.
- [11] S. Shellhammer, B. Tian, and R. van Nee, "WUR power spectral density," IEEE 802.11-18/0824, May 2018.
- [12] J. Jia Jia *et al.*, "WUR preamble sequence design and performance evaluation," IEEE 802.11-18/0435, 2018.
- [13] "Part 11: Wireless LAN medium access control (MAC) and physical layer (PHY) specifications," *IEEE Std 802.11-2016 (Revision of IEEE Std 802.11-2012)*, pp. 1–3534, Dec. 2016.
- [14] M. Golay, "Complementary series," *IRE Trans. Inf. Theory*, vol. 7, no. 2, pp. 82–87, Apr. 1961.
- [15] M. G. Parker, K. G. Paterson, and C. Tellambura, "Golay complementary sequences," in *Wiley Encyclopedia of Telecommunications*, 2003.
- [16] A. Sahin and R. Yang, "A reliable uplink control channel design with complementary sequences," in *Proc. IEEE International Conference on Communications (ICC)*, May 2019.
- [17] W. H. Holzmann and H. Kharaghani, "A computer search for complex Golay sequences," *Aust. Journ. Comb.*, vol. 10, pp. 251–258, Apr. 1994.